Hypertension
Journal of the American Heart Association

Cardiotrophin 1 Is Involved in Cardiac, Vascular, and Renal Fibrosis and Dysfunction

Natalia López-Andrés, Amélie Rousseau, Riaz Akhtar, Laurent Calvier, Carmen Iñigo, Carlos Labat, Xuegen Zhao, Kennedy Cruickshank, Javier Díez, Faiez Zannad, Patrick Lacolley and Patrick Rossignol

Hypertension. 2012;60:563-573; originally published online June 25, 2012;
doi: 10.1161/HYPERTENSIONAHA.112.194407
Hypertension is published by the American Heart Association, 7272 Greenville Avenue, Dallas, TX 75231

Print ISSN: 0194-911X. Online ISSN: 1524-4563

Cardiotrophin 1 Is Involved in Cardiac, Vascular, and Renal Fibrosis and Dysfunction

Natalia López-Andrés, Amélie Rousseau, Riaz Akhtar, Laurent Calvier, Carmen Iñigo, Carlos Labat, Xuegen Zhao, Kennedy Cruickshank, Javier Díez, Faiez Zannad, Patrick Lacolley, Patrick Rossignol

Abstract—Cardiotrophin 1 (CT-1), a cytokine belonging to the interleukin 6 family, is increased in hypertension and in heart failure. We aimed to study the precise role of CT-1 on cardiac, vascular, and renal function; morphology; and remodeling in early stages without hypertension. CT-1 (20 μg/kg per day) or vehicle was administrated to Wistar rats for 6 weeks. Cardiac and vascular functions were analyzed in vivo using M-mode echocardiography, Doppler, and echo tracking device and ex vivo using a scanning acoustic microscopy method. Cardiovascular and renal histomorphology were measured by immunohistochemistry, RT-PCR, and Western blot. Kidney functional properties were assessed by serum creatinine and neutrophile gelatinase-associated lipocalin and microalbuminuria/creatininuria ratio. Without alterations in blood pressure levels, CT-1 treatment increased left ventricular volumes, reduced fractional shortening and ejection fraction, and induced myocardial dilatation and myocardial fibrosis. In the carotid artery of CT-1–treated rats, the circumferential wall stress-incremental elastic modulus curve was shifted leftward, and the acoustic speed of sound in the aorta was augmented, indicating increased arterial stiffness. Vascular media thickness, collagen, and fibronectin content were increased by CT-1 treatment. CT-1–treated rats presented unaltered serum creatinine concentrations but increased urinary and serum neutrophile gelatinase-associated lipocalin and microalbuminuria/creatininuria ratio. This paralleled a glomerular and tubulointerstitial fibrosis accompanied by renal epithelial-mesenchymal transition. CT-1 is a new potent fibrotic agent in heart, vessels, and kidney able to induce cardiovascular-renal dysfunction independent from blood pressure. Thus, CT-1 could be a new target simultaneously integrating alterations of heart, vessels, and kidney in early stages of heart failure. **(*Hypertension*. 2012;60:563-573.)** ● **Online Data Supplement**

Key Words: cardiotrophin 1 ■ fibrosis ■ ventricular function ■ arterial stiffness ■ renal dysfunction

Heart failure (HF) is associated with cardiac hypertrophy, fibrosis, arterial stiffness, and renal impairment, all of which influence cardiovascular outcomes.[1–3] Cardiac hypertrophy is attributable to cardiomyocyte hypertrophy, the proliferation of interstitial fibroblasts, and increased depositions of extracellular matrix (ECM) components.[4] Arterial stiffening is associated with decreased distensibility and modified wall structure mainly characterized by increased ECM.[5,6] Chronic kidney disease progression is generally associated with tubulointerstitial fibrosis.[7,8] Therefore, it is of paramount importance to identify common pathways able to trigger cardiovascular and renal fibrosis.

Cardiotrophin 1 (CT-1) is an interleukin 6 superfamily member.[9] Elevated CT-1 levels have been reported in HF and in hypertensive patients.[10–12] Moreover, CT-1 positively correlates with left ventricular (LV) mass index and the serum concentration of carboxy-terminal propeptide of procollagen type I, a biomarker of collagen synthesis,[10] suggesting that CT-1 may contribute to the development of cardiomyocyte hypertrophy and fibrosis. Accordingly, CT-1 administration increases heart weight in mice.[13] Our group has characterized CT-1–induced cardiomyocyte survival and hypertrophy,[10,14] as well as CT-1–induced proliferation, hypertrophy, and secretion of ECM proteins in vascular smooth muscle cells (VSMCs).[15] Furthermore, CT-1 stimulates proliferation and collagen synthesis in ventricular fibroblasts.[16] In addition, the expression of CT-1 mRNA has been described in the kidney,[17] and mice treated with CT-1 showed increased renal weight.[13] Although these observations suggest that CT-1 may directly induce cardiac, vascular, and renal remodeling, no studies have directly investigated an integrative role of CT-1 in mediating fibrosis or cardiac, vascular, and renal dysfunc-

Received March 5, 2012; first decision April 2, 2012; revision accepted May 14, 2012.

From the Institut National de la Santé et de la Recherche Médicale U961 (N.L.-A., A.R., L.C., C.L., F.Z., P.L.). Vandoeuvre-lès-Nancy, France; School of Engineering (R.A.), University of Liverpool, Liverpool, United Kingdom; Division of Cardiovascular Sciences, Centre for Applied Medical Research (C.I., J.D.), and Department of Cardiology and Cardiac Surgery, University Clinic (J.D.), University of Navarra, Pamplona, Spain; School of Materials (X.Z.), University of Manchester, Manchester, United Kingdom; King's College (K.C.), London, United Kingdom; Institut National de la Santé et de la Recherche Médicale Clinical Investigation Centre (F.Z., P.R.), CIC9501, Vandoeuvre-lès-Nancy, France.

The online-only Data Supplement is available with this article at http://hyper.ahajournals.org/lookup/suppl/doi:10.1161/HYPERTENSIONAHA.112.194407/-/DC1.

Correspondence to Natalia López-Andrés, Institut National de la Santé et de la Recherche Médicale U961, Faculty of Medicine, Vandoeuvre-lès-Nancy, France. E-mail nlopand@alumni.unav.es

Hypertension **is available at http://hyper.ahajournals.org** **DOI: 10.1161/HYPERTENSIONAHA.112.194407**

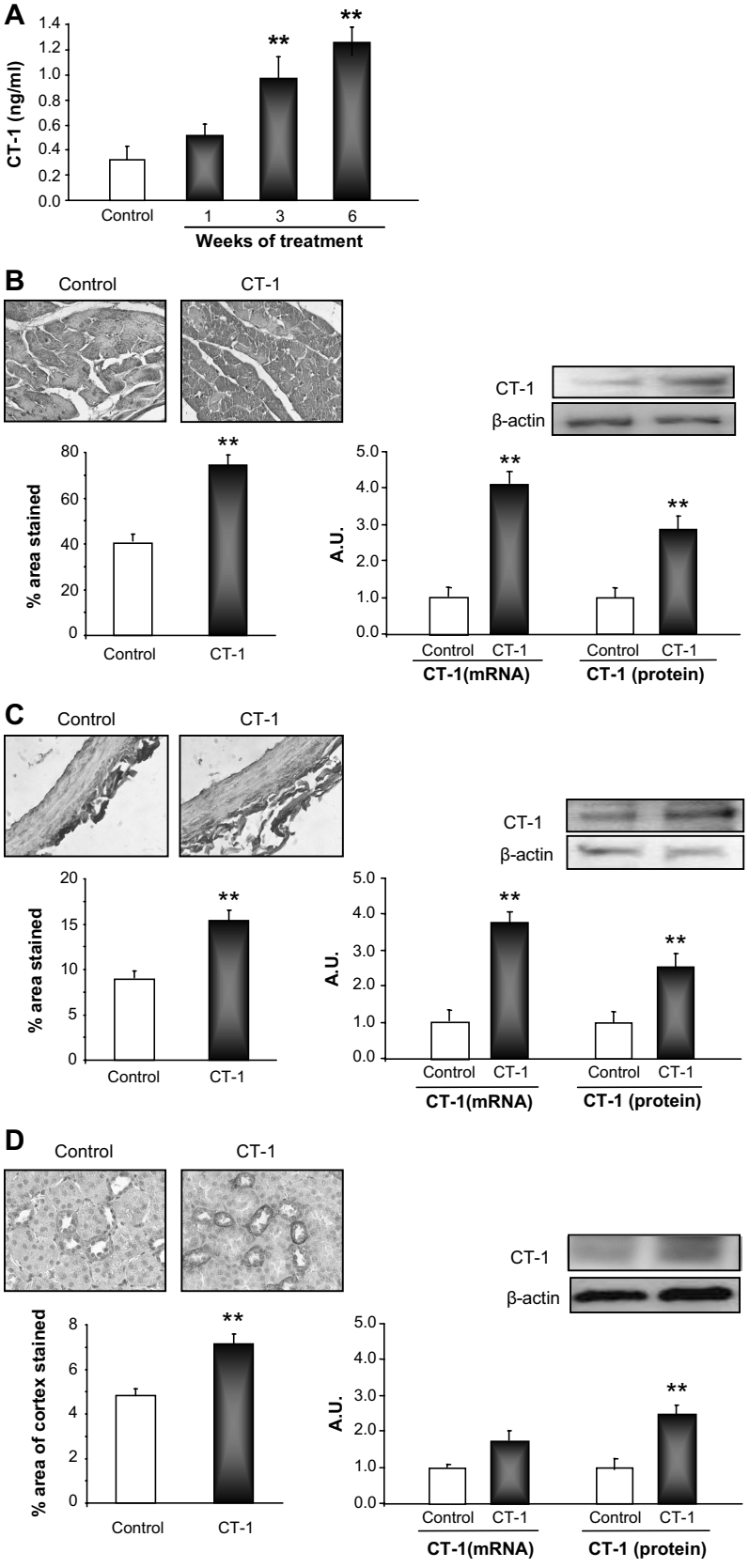

Figure 1. Cardiotrophin 1 (CT-1) levels in control and CT-1–treated rats. **A**, CT-1 treatment induced a time-dependent increase in CT-1 plasma levels. **B** through **D**, CT-1 expression, at the protein and the mRNA level, was enhanced in myocardium, the aorta, and the kidney from CT-1–treated rats. 18s gene expression or β-actin levels were used as loading controls in RT-PCR and Western blot, respectively. Values are mean±SEM; $^{**}P<0.01$ vs control.

tion in vivo. Therefore, we aimed to examine the precise role of CT-1 on cardiac, vascular, and renal functions; morphologies; and remodeling in rats chronically treated with CT-1.

Methods

Please see the online-only Data Supplement.

Animals

The investigation was performed in accordance with the Guide for Care and Use of Laboratory Animals published by the National Institutes of Health (publication No. 82-23, revised in 1996). Male Wistar rats (15 weeks old) were obtained from Harlan and treated with rat recombinant CT-1 (20 μg/kg per day, IP; n=30) or vehicle (PBS, IP; n=30) for 6 weeks and euthanized by decapitation under anesthesia (3% isofluorane/O_2).

Blood Pressure Monitoring

The surgical procedure for transmitter implantation was performed as described previously.[18]

Assessment of Ventricular Size and Heart Function

2D echocardiography, M-mode measurements, and Doppler ultrasound recordings were performed as described previously.[19]

In Vivo Carotid Mechanical Properties

We recorded intra-arterial diameter of the carotid artery and blood pressure (BP) as, described previously.[20]

Ex Vivo Aorta Mechanical Properties

Scanning acoustic microscopy (SAM), conducted at 761 MHz, was used to generate speed of sound maps for aorta sections using a novel method[21] but using the same sample preparation method, as described previously.[22] Any differential contribution to stiffness within the aortic wall was investigated by determining the speed of sound for both the elastic lamellae and interlamellar regions.[23]

Aortic Composition

Insoluble elastin, total collagen, and cell protein contents were measured on descending thoracic aortas without homogenization, as described previously.[24]

Histological Evaluation

Histological determinations in cardiac, vascular, and renal tissue were performed as described previously.[18]

Reverse Transcription and Real-Time PCR

Total RNA extraction and real-time PCR were performed as described previously.[18]

Western Blot

Western Blot analysis in left ventricles, aortas, and kidneys were performed as described previously.[18]

Zymography

Gelatin zymography for matrix metalloproteinase (MMP) activity assay was performed as described previously.[15]

Table. Cardiac, Vascular, and Renal Functions in Controls and CT-1–Treated Rats

Parameter	Control	CT-1
N	10	10
BW, g	265±6	278±5
HW, g	0.593±0.01	0.677±0.01*
HW/BW, mg · g^{-1}	2.25±0.07	2.45±0.08
KW, g	1.95±0.05	2.15±0.08*
KW/BW, mg · g^{-1}	7.39±0.23	7.76±0.32
SBP, mm Hg	135±7	133±6
DBP, mm Hg	90±6	84±6
MBP, mm Hg	105±6	100±6
PP, mm Hg	45±2	49±3
HR, bpm	426±11	404±10
Echocardiographic parameters		
LVMI, mg · g^{-1}	1.136±0.04	1.145±0.03
LVDd, mm	5.3±0.2	5.8±0.2*
LVSd, mm	3.0±0.3	3.8±0.2*
LVDv, mL	0.37±0.02	0.47±0.05*
LVSv, mL	0.09±0.02	0.15±0.03*
FS, %	44.0±3.3	34.0±3.0*
EF, %	79.5±3.1	69.3±3.9*
E/A	1.42±0.04	1.60±0.04*
Vascular parameters, at MBP		
Carotid diameter, mm	1.20±0.05	1.03±0.03*
Carotid compliance	8.1±0.7	6.5±0.6
Distensibility, 10^{-3}mm Hg^{-1}	7.5±0.9	7.9±0.7
Incremental elastic modulus, kPa	749±166	362±36*
Wall stress, kPa	298±37	154±14*
Renal parameters		
S_{Cr}, pg/mL	0.174±0.002	0.176±0.003
S_{Alb}, pg/mL	241±10	405±109
S_{NGAL}, ng/mL	43±7	83±16*
U_{Cr}, pg/mL	1.94±0.06	2.01±0.06
U_{Alb}, pg/mL	2359±370	3349±355*
ACR, μg/μg creatinine	1.21±0.20	1.75±0.17*
U_{NGAL}, ng/mL	176±2	362±51*

BW indicates body weight; HW, heart weight; KW, kidney weight; SBP, systolic blood pressure; DBP, diastolic blood pressure; MBP, mean blood pressure; PP, pulse pressure; HR, heart rate; LVDd, left ventricular end-diastolic diameter; LVSd, left ventricular end-systolic diameter; LVDv, left ventricular diastolic volume; LVSv, left ventricular systolic volume; FS, fractional shortening; EF, left ventricular ejection fraction; E/A, ratio E wave and A wave mitral flow; S_{Cr}, serum creatinine; S_{Alb}, serum albumin; S_{NGAL}, serum neutrophile gelatinase-associated lipocalin; U_{Cr}, urinary creatinine; U_{Alb}, urinary albumin; ACR, albumin-to-creatinine ratio; U_{NGAL}, urinary neutrophile gelatinase-associated lipocalin.

*$P<0.01$ vs control.

ELISA

Quantikine ELISA kits were used to measure albumin and creatinine (Abnova), neutrophile gelatinase-associated lipocalin (Interchim), and CT-1 (Cusabio) according to the manufacturer's protocols.

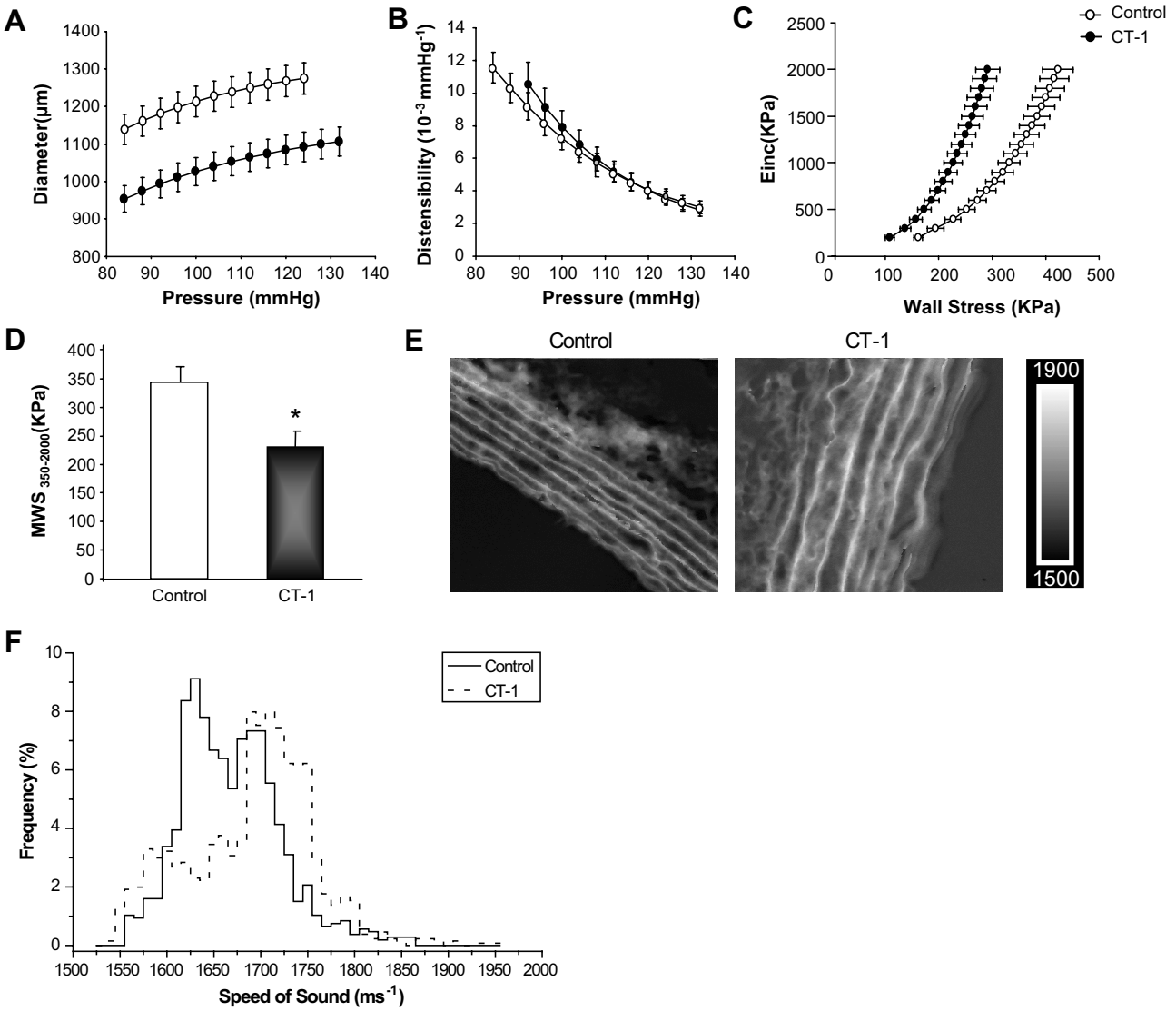

Figure 2. In vivo and ex vivo vascular mechanical properties in control and cardiotrophin 1 (CT-1)–treated rats. **A**, The diameter-arterial pressure curve of the CT-1–treated group (n=9) was significantly shifted downward versus controls (n=9). **B**, No difference in arterial distensibility was observed between the 2 groups. **C**, The wall stress (WS)- incremental elastic modulus (E_{inc}) curve of CT-1–treated rats was significantly shifted to the left versus controls. **D**, Mean WS (MWS) within the 350- to 2000-KPa range of E_{inc} (MWS 350-2000) was decreased in CT-1–treated rats. **E** and **F**, 200×200-μm speed of sound maps for a typical control and CT-1–treated rat aorta determined with scanning acoustic microscopy (SAM). N=1000 speed of sound measurements per group. Values are mean±SEM. *P<0.05 vs control; **P<0.01 vs control. **A** through **C**, ○, control; ●, CT-1. **F**, Black line, control; dashed line, CT-1.

Statistical Analysis

Results are presented as mean±SEM, and P values <0.05 were considered significant. Comparisons between treatments or groups of animals were made by the unpaired Student t test, the Mann-Whitney U test, or the repeated-measures ANOVA, as appropriate.

Results

CT-1 Levels in CT-1–Treated Rats

CT-1 plasma levels were measured at baseline and at 1, 3, and 6 weeks of treatment. As shown in Figure 1A, CT-1 levels were increased at 3 (2.8-fold; P<0.01) and 6 weeks of injection (3.8-fold; P<0.01).

CT-1 was spontaneously expressed in cardiac tissue, both in cardiomyocytes and fibroblasts. Moreover, CT-1–treated rats presented higher (70%; P<0.01) CT-1 immunostaining as compared with controls. This increase was confirmed at the mRNA (4.1-fold; P<0.01) and the protein (2.8-fold; P<0.01) levels (Figure 1B). CT-1 was also expressed in aortic VSMCs. The expression was higher (80%; P<0.01) in CT-1-treated animals. The cytokine was also enhanced at the mRNA (3.7-fold; P<0.01) and the protein (2.3-fold; P<0.01) levels in aorta from CT-1–treated rats (Figure 1C). In kidney, CT-1 was spontaneously localized in the distal tubular cells of the cortex but not in glomeruli. CT-1 expression was higher (48%; P<0.01) in renal cortex from CT-1–treated animals. Moreover, CT-1 expression was increased at the protein level (2.3-fold; P<0.01) but not significantly at the mRNA level in kidney from CT-1–infused rats relative to controls (Figure 1D). The expression of CT-1 receptors gp130 and Leukemia inhibitory factor receptor was also evaluated in heart, aorta, and kidney (please see Figure S1).

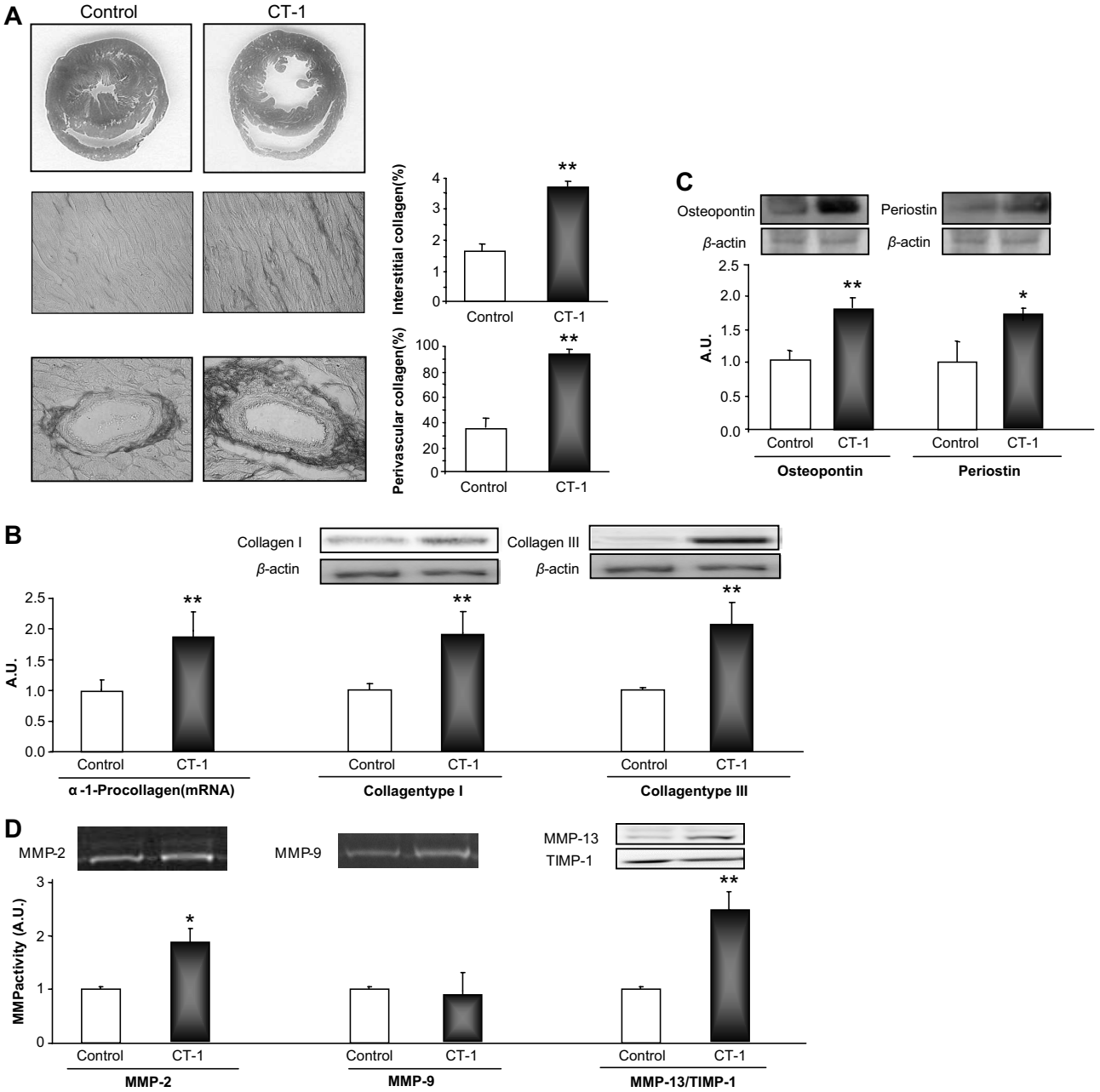

Figure 3. Cardiac morphology and composition in controls and cardiotrophin 1 (CT-1)–treated rats. **A**, CT-1–treated rats presented left ventricular (LV) chamber dilatation and interstitial and perivascular fibrosis. **B** and **C**, The expression of the extracellular matrix (ECM) components was quantified by RT-PCR and Western blot in the myocardium from controls (n=10) and CT-1–treated rats (n=10). 18s gene expression or β-actin levels were used as loading controls in RT-PCR and Western blot, respectively. CT-1–treated rats presented increased cardiac α-1-procollagen, collagen type I, collagen type III, osteopontin, and periostin. **D**, CT-1–treated rats exhibited cardiac activation of MMP-2 and -13. Representative images are shown, and the histogram bars represent the mean±SEM obtained in the 2 groups of animals. *$P<0.05$ vs control; **$P<0.01$ vs control.

Cardiac, Vascular, and Renal Functions in CT-1–Treated Rats

Chronic CT-1 administration had no effect on BP parameters throughout the experimental period. The heart weight/body weight ratio was not significantly different in the 2 groups, indicating a similar LV mass index (Table).

Echocardiographic analysis confirmed that LV mass index was similar in the 2 groups. CT-1 administration increased ($P<0.01$) systolic and diastolic LV diameters and volumes. CT-1–treated rats exhibited LV chamber dilatation (representative images are shown in Figure 3A). CT-1–treated rats presented decreased ($P<0.01$) fractional shortening and ejection fraction as compared with controls and increased E/A ratio ($P<0.01$), suggesting a trend toward restrictive filling (Table). The ratio between end-systolic volume and stroke volume was increased by CT-1 treatment (36%; $P<0.01$), suggesting that CT-1 impaired LV-arterial coupling.

Ultrasonic echo tracking assessment revealed that the carotid diameter was smaller in CT-1–treated rats than in the controls (Table). There were no significant differences in

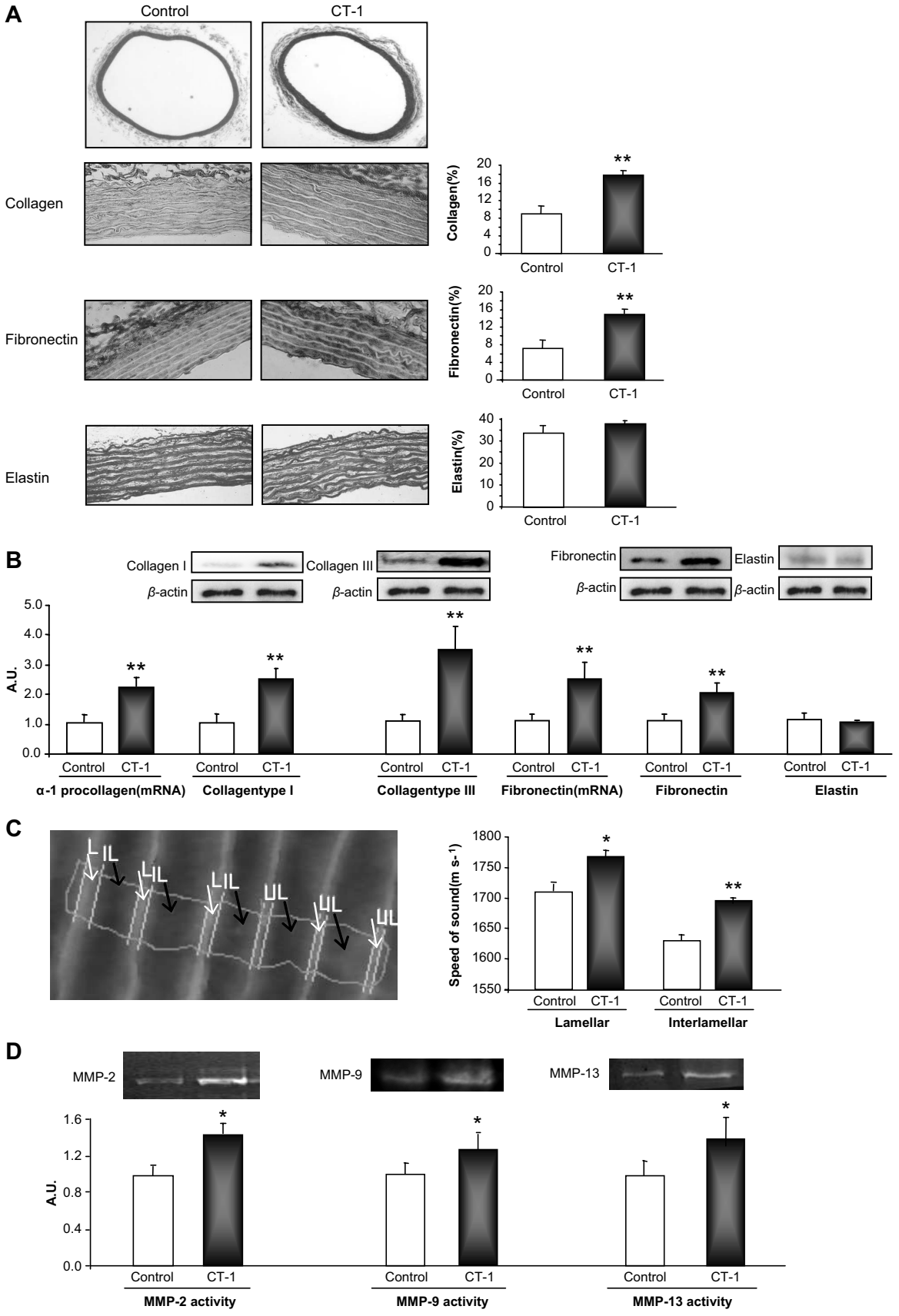

Figure 4. Vascular morphology and composition in controls and cardiotrophin 1 (CT-1)–treated rats. **A**, Carotid artery from CT-1–treated rats exhibited increased media cross-sectional area of the carotid artery (MCSA), collagen, and fibronectin contents, whereas elastin levels were not modified. **B**, CT-1–treated rats presented increased aortic α-1-procollagen mRNA, collagen type I, collagen type

compliance and distensibility calculated at the mean BP. Incremental elastic modulus and wall stress were lower in CT-1–treated rats compared with controls. Within the common range of arterial pressure, the diameter-arterial pressure curve in the CT-1–treated group was significantly shifted downwards from that of the control group (Figure 2A). The distensibility-arterial pressure curve was similar in the 2 groups (Figure 2B). By contrast, the incremental elastic modulus-WS curve of CT-1–treated rats was shifted leftward significantly (Figure 2C). Accordingly, in CT-1–treated rats the mean WS within the 350- to 2000-kPa range of incremental elastic modulus was decreased ($P<0.01$), indicating an increase in stiffness (Figure 2D). Typical SAM speed of sound maps for the aorta samples are shown in Figure 2E and 2F. Mean speed of sound in the CT-1–treated rats was found to increase significantly ($P<0.01$), confirming increased arterial stiffness.

The kidney weight/body weight ratio was not significantly different in both groups (Table). At the end of the treatment, CT-1–treated rats presented enhanced (44%; $P<0.05$) albumin-creatinine ratio as compared with controls. Furthermore, neutrophile gelatinase-associated lipocalin, a tubular injury biomarker, was increased in serum from CT-1–treated rats (93%; $P<0.05$), as well as in urine (234%, $P<0.05$), as compared with controls.

Myocardial, Vascular, and Renal Fibrosis in CT-1–Treated Rats

Myocardial Fibrosis

CT-1 treatment increased cardiomyocyte length (14%; $P<0.01$), without modifying cardiomyocyte width. Moreover, CT-1 treatment induced the expression of the contractile proteins α-major histocompatibility complex, β-major histocompatibility complex, α-sarcomeric actin, and myosin light chain 1 without modifying α-skeletal actin or myosin light chain 2v levels (please see Figure S2).

CT-1–infused rats presented a 2-fold increase ($P<0.01$) in cardiac interstitial collagen and a 2.5-fold increase ($P<0.01$) in perivascular collagen (Figure 3A) as compared with controls. CT-1–treated rats showed higher cardiac expression of α-1-procollagen mRNA (80%; $P<0.01$), collagen type I (80%; $P<0.01$), and type III (2-fold; $P<0.01$; Figure 3B). Moreover, CT-1–treated rats exhibited higher levels of osteopontin (75%; $P<0.01$) and periostin (65%; $P<0.05$; Figure 3C). CT-1–treated rats presented enhanced MMP-2 activity (80%; $P<0.05$), as well as MMP-13/tissue inhibitor of metalloproteinase 1 ratio (2.4-fold; $P<0.01$), without significant changes in MMP-9 activity (Figure 3D).

Vascular Fibrosis

Media thickness and media cross-sectional area of the carotid artery were higher (41% and 43%, respectively; $P<0.01$), whereas carotid diameter was reduced by 15% ($P<0.01$) in CT-1–treated animals as compared with controls (Figure S3, and representative images are shown in Figure 4A).

Thoracic aortic medial dry weight per centimeter of length and cell protein content were increased significantly by the CT-1 treatment compared with control rats (Figure S3), indicating that hypertrophy of the media had occurred. There were no changes in elastin with CT-1 treatment. However, CT-1–treated rats presented enhanced aortic collagen content (30% to 50%; $P<0.01$) as compared with controls.

To determine whether CT-1 could modify ECM attachments, integrins expression was studied. CT-1 treatment increased the expression of the integrins α-1, α-5, α-v, and β-3. To analyze whether CT-1 also modified the cytoskeletal proteins involved in linkage to integrin adhesion molecules to the actin cytoskeleton, we quantified the phosphorylation of focal adhesion kinase and the expression of 2 focal adhesions proteins, vinculin and talin. Aortas from CT-1–treated rats exhibited enhanced expression of vinculin and talin, as well as greater focal adhesion kinase activity (Figure S3).

CT-1–treated rats had higher carotid collagen (80%; $P<0.01$) and enhanced fibronectin (80%; $P<0.01$) but similar elastin densities compared with controls (Figure 4A). Moreover, in aorta from CT-1–treated rats, the expression of α-1-procollagen mRNA was higher (2.1-fold; $P<0.01$), as well as the expression of collagen type I (2.4-fold; $P<0.01$) and type III (3.6-fold; $P<0.01$; Figure 4B). In addition, CT-1–administrated rats presented enhanced aortic fibronectin content at the mRNA (2.4-fold; $P<0.01$) and the protein (80%; $P<0.01$) levels but similar content of elastin compared with controls (Figure 4B).

The SAM images were also analyzed to determine whether there was any localized stiffening by examining the speed of sound in the lamellar and interlamellar regions of the aorta. There was a significant increase in stiffness in both lamellar and interlamellar regions; however, the interlamellar regions exhibited the most significant change in the CT-1–treated rats (Figure 4C). This is consistent with the increase in collagen content (Figure 4A and 4B), which would be expected to accumulate more in the interlamellar regions. Aortas from CT-1–treated rats showed enhanced MMP-2 (40%; $P<0.05$), MMP-9 (20%; $P<0.05$), and MMP-13 (30%; $P<0.05$) activities as compared with controls (Figure 4D).

Renal Fibrosis

CT-1–infused rats presented increased (49%; $P<0.01$) renal interstitial collagen as compared with controls. Moreover, glomerular collagen volume fraction in CT-1–treated rats was markedly increased (72%; $P<0.01$). Tubulointerstitial collagen type I and type IV were higher (240% and 260%; $P<0.01$, respectively) in CT-1–treated animals (Figure 5A). This was confirmed by molecular analysis (Figure 5B). In

Figure 4 (Continued). III, and fibronectin, whereas elastin levels were similar. **C**, **left**, 2D analysis of scanning acoustic microscopy (SAM) images; the lamellar and interlamellar regions of the aorta are demarcated, after which the speed of sounds (stiffness) values are extracted for each of these regions. **Right**, There is a significant increase in both the lamellar (L) and interlamellar (IL) regions of the aorta, with the most prominent changes being in the interlamellar region (n=33, L and IL per group). **D**, In aorta from CT-1–treated rats there was an activation of MMP-2, -9, and -13. Representative images are shown, and the histogram bars represent the mean±SEM obtained in the 2 groups of animals. *$P<0.05$ vs control. **$P<0.01$ vs control.

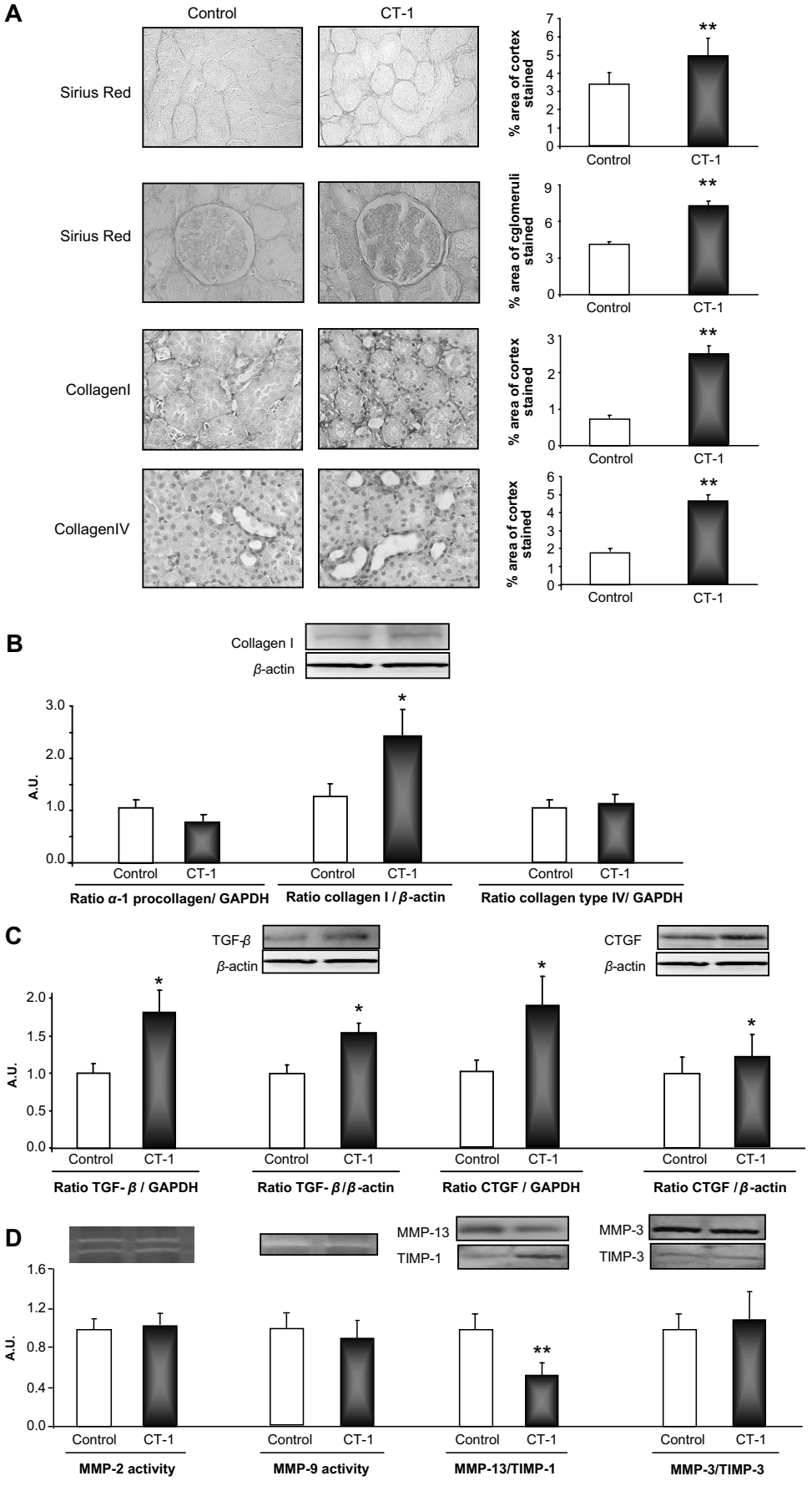

addition, CT-1–administrated rats presented enhanced expression of transforming growth factor-β_1 (84% to 55%; $P<0.05$) and connective tissue growth factor (87% to 21%; $P<0.05$) at the mRNA and protein levels, respectively (Figure 5C). MMP-9 and MMP-2 activities and MMP-3/tissue inhibitor of metalloproteinase 3 ratio were similar in the kidneys from the 2 groups of rats, whereas the MMP-13/tissue inhibitor of metalloproteinase 1 ratio was decreased in CT-1–treated animals (64%; $P<0.01$; Figure 5D).

Discussion

The purpose of this study was to investigate the influence of an excess of circulating CT-1 in cardiac, vascular, and renal remodeling and function in rats. Indeed, in the absence of BP modifications, chronic CT-1 treatment induced cardiac, vascular, and renal fibrosis, resulting in further structural and functional damage in heart, aorta, and kidney. Moreover, increased CT-1 mRNA expression observed in the cardiovascular system from CT-1–treated rats suggests a positive feedback inducing a vicious circle.

Hypertension, HF, and chronic kidney disease have been shown to be associated with increased CT-1 plasma levels,[10,11,14,25,26] with these being increases similar to those found in the present study. Furthermore, CT-1 treatment weakens cardiomyocyte contractility in reconstituted heart tissue,[27] suggesting a role for CT-1 in the impairment of cardiac function. However, the precise contribution of CT-1 to the pathogenesis of cardiac remodeling and dysfunction is unclear, because, to our knowledge, the in vivo CT-1 effects have not yet been investigated. CT-1 induced cardiomyocyte hypertrophy in vitro, with a special morphometric pattern of lengthening without modifying cell width and without changing α-skeletal actin or myosin light chain 2v expression.[14] CT-1 also increased collagen synthesis in fibroblasts.[16] Our study showed that CT-1–treated rats developed LV dilatation accompanied by cardiomyocyte elongation, produced by an increase in contractile proteins except for α-skeletal actin and myosin light chain 2v, as well as enhanced myocardial fibrosis characterized by ECM protein deposition. In addition, CT-1 treatment decreased LV mechanical efficiency by modulating the heart-vessel coupling, independent of BP. Thus, direct structural changes produced by CT-1, cardiomyocyte lengthening, and myocardial fibrosis could contribute overall to cardiac dysfunction and LV-arterial uncoupling.

In addition to cardiac fibrosis and dysfunction, CT-1 induced significant vascular remodeling characterized by ECM proteins accumulation and arterial stiffness. We have shown recently that CT-1 increases proliferation, ECM synthesis, and hypertrophy in VSMCs.[15] The molecular mechanisms underlying the development of vascular stiffness are generally attributed to modifications in ECM molecules, VSMC changes, and vascular tone.[28,29] Interestingly, chronic CT-1 treatment reduced arterial diameter and increased media cross-sectional area of the carotid artery in vessels, with a marked deposition of ECM proteins, integrins, and focal adhesion molecules. These modifications may represent quantitative or topographical changes in interactions between VSMCs and matrix proteins, resulting in a restructured vascular wall, as described previously in other models.[28,29] With the novel SAM technique, we found an increase in speed of sound of 29 ms^{-1} in the CT-1–treated rat aorta. This is much higher than the age-related increase reported with a SAM method for ovine aorta,[23] thereby highlighting the profound effect of CT-1 on vascular stiffening. The increased stiffness determined with SAM ex vivo on thin sections of tissue follows the trends observed with more conventional techniques in vivo, providing high spatial resolution measurements of stiffness, which are related to tissue structure. Consequently, these findings provide additional evidence suggesting that CT-1 may contribute to increase the arterial stiffness, ultimately leading to vascular dysfunction.

In kidney, only the expression of CT-1 mRNA has been described to date.[17] Moreover, mice treated with CT-1 showed increased renal weight.[13] Consistent with observations in myocardium and vessels, CT-1–treated rats presented increased tubulointerstitial and glomerular fibrosis, accompanied by enhanced transforming growth factor-β and connective tissue growth factor expressions, 2 molecules that act synergistically to promote kidney fibrosis.[30] Moreover, CT-1 has the ability to alter the differentiation state of tubular epithelial cells toward an EMT phenotype, which ultimately generates fibrosis and dysfunction. CT-1 also altered kidney functional properties, inducing albuminuria and increasing urinary and serum neutrophile gelatinase-associated lipocalin, an immediate early gene, which is associated with chronic kidney disease progression.[31] Taken together, these data indicate that chronic CT-1 exposure plays a role in renal fibrosis and tubular damage in vivo.

Conclusion and Perspectives

This experimental model of chronic CT-1 exposure presents integrated early changes of heart, artery, and kidney functions, which may ultimately lead to HF development. Of interest, our study identifies new important direct effects of CT-1 in the absence of BP modifications. Previous studies demonstrated that CT-1 may be stimulated by hypertension and by aldosterone even in the absence of BP elevation.[18] In the present study, CT-1 levels were similar to those observed in human HF,[10–12] and, moreover, CT-1 infusion was associated with increased CT-1 transcription in heart and vessels,

Figure 5 (Continued). Renal fibrosis in control and cardiotrophin 1 (CT-1)–treated rats. **A**, Total tubulointerstitial and glomerular collagen content, tubulointerstitial collagen type I, and collagen type IV were increased in kidney from CT-1–treated rats, as compared with controls. **B**, Collagen type I expression was augmented, whereas the expression of α-1 procollagen and collagen type IV mRNA was unchanged in kidney from CT-1–treated rats as compared with controls. **C**, Transforming growth factor (TGF)-β_1 and connective tissue growth factor (CTGF) mRNA and protein expression were enhanced in whole kidney tissue from rats treated with CT-1 as compared with controls. **D**, In kidney from CT-1–treated rats there was a decrease in matrix metalloproteinase (MMP) 13 activity. GAPDH expression or β-actin levels are used as loading controls in RT-PCR and Western blot, respectively. Bars represent the mean±SEM obtained in the 2 groups of animals. *$P<0.05$ vs control; **$P<0.01$ vs control.

thereby suggesting a positive feedback loop able to promote further CT-1 effects. Therefore, CT-1, per se, could be an additional therapeutic target downstream to many ischemia-derived neurohumoral influences involved in HF pathophysiology. There is currently no way to inhibit CT-1 in vivo. Finally, we suggest that CT-1 emerges as a target candidate to interfere with the development of cardiac-vascular-renal fibrosis and dysfunction that characterizes cardiovascular-renal diseases evolving with HF.

Acknowledgments

We especially thank Prof Simon Thornton for editing this article, and Ginny Simon, Natacha Sloboda, and Patrick Costello for technical assistance. Prof Brian Derby must be thanked for leading the development of the SAM technique under the Wellcome Trust grant WT085981AIA, along with Drs Michael Sherratt and Rachel Watson. We thank Dr Sebastian Brand (Fraunhofer Institute of Material Mechanics, Germany) and Prof Kay Raum (Julius Wolff Institut and Berlin-Brandenburg School for Regenerative Therapies, Germany), who developed the MATSAM software. We also thank Drs Maria Antonia Fortuno, Pascal Challande, Mary Osborne, and Jean-Paul Duong Van Huyen for helpful discussion.

Sources of Funding

This work was supported by a grant from the Institut National de la Santé et de la Recherche Médicale, the Programme National de Recherche Cardiovasculaire, La Société Française d'Hypertension artérielle, la Région Lorraine, the Sixth European Union-Framework Program Network of Excellence "Ingenious HyperCare" (contract No. LSHM-CT-2006-037093), the agreement between the Foundation for Applied Medical Research and Union Temporal de Empresas, University of Navarra, and the Seventh European Union-Framework Program MEDIA project (261409). R.A. is grateful to the British Heart Foundation for funding (FS/08/036/25364) and X.Z. to the Wellcome Trust (WT085981AIA).

Disclosures

None.

References

1. Shirwany NA, Zou MH. Arterial stiffness: a brief review. *Acta Pharmacol Sin*. 2010;31:1267–1276.
2. Smith GL, Lichtman JH, Bracken MB, Shlipak MG, Phillips CO, DiCapua P, Krumholz HM. Renal impairment and outcomes in heart failure: systematic review and meta-analysis. *J Am Coll Cardiol*. 2006; 47:1987–1996.
3. Swynghedauw B. Molecular mechanisms of myocardial remodeling. *Physiol Rev*. 1999;79:215–262.
4. Creemers EE, Pinto YM. Molecular mechanisms that control interstitial fibrosis in the pressure-overloaded heart. *Cardiovasc Res*. 2011;89: 265–272.
5. Intengan HD, Schiffrin EL. Vascular remodeling in hypertension: roles of apoptosis, inflammation, and fibrosis. *Hypertension*. 2001;38:581–587.
6. Lacolley P, Challande P, Osborne-Pellegrin M, Regnault V. Genetics and pathophysiology of arterial stiffness. *Cardiovasc Res*. 2009;81:637–648.
7. Harris RC, Neilson EG. Toward a unified theory of renal progression. *Annu Rev Med*. 2006;57:365–380.
8. Labban B, Arora N, Restaino S, Markowitz G, Valeri A, Radhakrishnan J. The role of kidney biopsy in heart transplant candidates with kidney disease. *Transplantation*. 2010;89:887–893.
9. Pennica D, King KL, Shaw KJ, Luis E, Rullamas J, Luoh SM, Darbonne WC, Knutzon DS, Yen R, Chien KR, Baker JB, Wood WI. Expression cloning of cardiotrophin 1, a cytokine that induces cardiac myocyte hypertrophy. *Proc Natl Acad Sci U S A*. 1995;92:1142–1146.
10. Gonzalez A, Lopez B, Martin-Raymondi D, Lozano E, Varo N, Barba J, Serrano M, Diez J. Usefulness of plasma cardiotrophin-1 in assessment of left ventricular hypertrophy regression in hypertensive patients. *J Hypertens*. 2005;23:2297–2304.
11. Lopez B, Gonzalez A, Querejeta R, Barba J, Diez J. Association of plasma cardiotrophin-1 with stage C heart failure in hypertensive patients: potential diagnostic implications. *J Hypertens*. 2009;27: 418–424.
12. Talwar S, Squire IB, Downie PF, O'Brien RJ, Davies JE, Ng LL. Elevated circulating cardiotrophin-1 in heart failure: relationship with parameters of left ventricular systolic dysfunction. *Clin Sci (Lond)*. 2000; 99:83–88.
13. Jin H, Yang R, Keller GA, Ryan A, Ko A, Finkle D, Swanson TA, Li W, Pennica D, Wood WI, Paoni NF. In vivo effects of cardiotrophin-1. *Cytokine*. 1996;8:920–926.
14. Lopez N, Diez J, Fortuno MA. Differential hypertrophic effects of cardiotrophin-1 on adult cardiomyocytes from normotensive and spontaneously hypertensive rats. *J Mol Cell Cardiol*. 2006;41:902–913.
15. Lopez-Andres N, Fortuno MA, Diez J, Zannad F, Lacolley P, Rossignol P. Vascular effects of cardiotrophin-1: a role in hypertension? *J Hypertens*. 2010;28:1261–1272.
16. Tsuruda T, Jougasaki M, Boerrigter G, Huntley BK, Chen HH, D'Assoro AB, Lee SC, Larsen AM, Cataliotti A, Burnett JC Jr. Cardiotrophin-1 stimulation of cardiac fibroblast growth: roles for glycoprotein 130/ leukemia inhibitory factor receptor and the endothelin type A receptor. *Circ Res*. 2002;90:128–134.
17. Ishikawa M, Saito Y, Miyamoto Y, Harada M, Kuwahara K, Ogawa E, Nakagawa O, Hamanaka I, Kajiyama N, Takahashi N, Masuda I, Hashimoto T, Sakai O, Hosoya T, Nakao K. A heart-specific increase in cardiotrophin-1 gene expression precedes the establishment of ventricular hypertrophy in genetically hypertensive rats. *J Hypertens*. 1999;17: 807–816.
18. Lopez-Andres N, Martin-Fernandez B, Rossignol P, Zannad F, Lahera V, Fortuno MA, Cachofeiro V, Diez J. A Role for cardiotrophin-1 in myocardial remodelling induced by aldosterone. *Am J Physiol Heart Circ Physiol*. 2011;301:H2372–H2382.
19. Agbulut O, Coirault C, Niederlander N, Huet A, Vicart P, Hagege A, Puceat M, Menasche P. GFP expression in muscle cells impairs actin-myosin interactions: implications for cell therapy. *Nat Methods*. 2006; 3:331.
20. Lacolley P, Labat C, Pujol A, Delcayre C, Benetos A, Safar M. Increased carotid wall elastic modulus and fibronectin in aldosterone-salt-treated rats: effects of eplerenone. *Circulation*. 2002;106:2848–2853.
21. Zhao X, Akhtar R, Nijenhuis N, Wilkinson SJ, Murphy L, Ballestrem C, Sherratt MJ, Watson REB, Derby B. Multi-layer phase analysis: quantifying the elastic properties of soft tissues and live cells with ultra-high-frequency scanning acoustic microscopy. *IEEE Trans Ultrason Ferroelectr Freq Control*. 2012;59:610–620.
22. Akhtar R, Sherratt MJ, Watson RE, Kundu T, Derby B. Mapping the micromechanical properties of cryo-sectioned aortic tissue with scanning acoustic microscopy. *Mater Res Soc Symp Proc*. 2009;1132E(1132-Z03-07):ukpmcpa27262.
23. Graham HK, Akhtar R, Kridiotis C, Derby B, Kundu T, Trafford AW, Sherratt MJ. Localised micro-mechanical stiffening in the ageing aorta. *Mech Ageing Dev*. 2011;132:459–467.
24. Qin W, Chung AC, Huang XR, Meng XM, Hui DS, Yu CM, Sung JJ, Lan HY. TGF-β/Smad3 signaling promotes renal fibrosis by inhibiting miR-29. *J Am Soc Nephrol*. 2011;22:1462–1474.
25. Cottone S, Nardi E, Mule G, Vadala A, Lorito MC, Riccobene R, Palermo A, Arsena R, Guarneri M, Cerasola G. Association between biomarkers of inflammation and left ventricular hypertrophy in moderate chronic kidney disease. *Clin Nephrol*. 2007;67:209–216.
26. Lopez N, Varo N, Diez J, Fortuno MA. Loss of myocardial LIF receptor in experimental heart failure reduces cardiotrophin-1 cytoprotection: a role for neurohumoral agonists? *Cardiovasc Res*. 2007; 75:536–545.
27. Zolk O, Engmann S, Munzel F, Krajcik R. Chronic cardiotrophin-1 stimulation impairs contractile function in reconstituted heart tissue. *Am J Physiol Endocrinol Metab*. 2005;288:E1214–E1221.
28. Bezie Y, Lacolley P, Laurent S, Gabella G. Connection of smooth muscle cells to elastic lamellae in aorta of spontaneously hypertensive rats. *Hypertension*. 1998;32:166–169.
29. Intengan HD, Thibault G, Li JS, Schiffrin EL. Resistance artery mechanics, structure, and extracellular components in spontaneously hypertensive rats: effects of angiotensin receptor antagonism and converting enzyme inhibition. *Circulation*. 1999;100:2267–2275.

30. Mori T, Kawara S, Shinozaki M, Hayashi N, Kakinuma T, Igarashi A, Takigawa M, Nakanishi T, Takehara K. Role and interaction of connective tissue growth factor with transforming growth factor-beta in persistent fibrosis: a mouse fibrosis model. *J Cell Physiol*. 1999;181:153–159.

31. Viau A, El Karoui K, Laouari D, Burtin M, Nguyen C, Mori K, Pillebout E, Berger T, Mak TW, Knebelmann B, Friedlander G, Barasch J, Terzi F. Lipocalin 2 is essential for chronic kidney disease progression in mice and humans. *J Clin Invest*. 2010;120:4065–4076.

Novelty and Significance

What Is New?

- We report the whole picture of CT-1 in vivo effects, with major insights into the profibrotic properties and the key role of CT-1 throughout the cardiovascular and renal continuum, ultimately leading to heart failure and kidney insufficiency.

What Is Relevant?

- First, we have characterized cardiac function, hypertrophy, and fibrosis induced by a chronic treatment with CT-1 in rats. Then, we provided data showing an increased arterial stiffness using classic methods, as well as a novel ultra-high frequency SAM phase contrast method that enables the determination of tissue elastic data within the aortic wall. Moreover, we present mechanistic insights regarding integrin expression and focal adhesion proteins in the aorta. Finally, we have explored CT-1 effects throughout the cardiovascular system, in renal tissue, presenting exciting data that suggest a key role for this molecule in the cardiovascular-renal syndrome. Our results are particularly original, because therapies that target the heart, the large arteries, and the kidney to directly reduce left ventricular dysfunction, arterial stiffness, and renal insufficiency are an important unmet clinical need.

Summary

CT-1 could be a new biotarget to reduce fibrosis, arterial stiffness, and cardiorenal dysfunction.

ONLINE SUPPLEMENT
CARDIOTROPHIN-1 IS INVOLVED IN CARDIAC, VASCULAR AND RENAL FIBROSIS AND DYSFUNCTION

Authors: López-Andrés Natalia [1], Rousseau Amélie[1], Akhtar Riaz [2], Calvier Laurent [1], Iñigo Carmen [3], Labat Carlos [1], Zhao Xuegen [4], Cruickshank Kennedy [5], Díez Javier [3,6], Zannad Faiez [1,7], Lacolley Patrick [1], Rossignol Patrick [1,7]

Affiliations: [1] Inserm, U961. Vandoeuvre-lès-Nancy, F-54505 (France); [2] School of Engineering, University of Liverpool, Liverpool (UK); [3] Division of Cardiovascular Sciences. Centre for Applied Medical Research. University of Navarra. Pamplona (Spain); [4] School of Materials, University of Manchester, Manchester (UK); [5] King's College, London (UK); [6] Department of Cardiology and Cardiac Surgery, University Clinic, University of Navarra, Pamplona (Spain); [7] Inserm Clinical Investigation Centre, CIC9501, Vandoeuvre-lès-Nancy (France)

Short title: Cardiotrophin-1 induced fibrosis

Corresponding Author:
Dr Natalia López-Andrés
Inserm, U961. Faculty of Medicine.
Vandoeuvre-lès-Nancy
Tel: +33 (0)3 83 68 36 25
Fax : +33 (0)3 83 68 36 39
e-mail: nlopand@alumni.unav.es

SUPPLEMENTARY METHODS

Animals

The investigation was performed in accordance with the Guide for Care and Use of Laboratory Animals published by the US National Institutes of Health *(NIH Publication NO.82-23, revised in 1996).* Male Wistar rats (15 weeks-old) were obtained from Harlan (Bicester, England) and treated with rat recombinant CT-1 (20 µg/kg/day, IP, n=30) or vehicle (PBS, IP, n=30) for 6 weeks. 15 animals per group were used for functional studies and 15 animals per group were used to complete the histological and the molecular determinations.

Blood pressure monitoring

The surgical procedure for transmitter implantation was performed in a sterilized area. Anaesthesia was induced with 3% isofluorane/O_2 and maintained during surgery with 1.5%. Telemetry transmitters (model TA11PA-C40; Data Sciences International) were implanted according to the manufacturer's indications (Data Sciences International), with RCP-1 receivers used for telemetric acquisition and analysis of systolic, diastolic, mean arterial pressure and heart rate (SBP, DBP, MAP and HR). The system was scheduled to obtain and store a 10 sec measurement every 15 minutes. Data were averaged in 24h intervals for posthoc analysis.

Assessment of ventricular size and heart function

Two-dimensional echocardiography, M-mode measurements and Doppler ultrasound recordings were performed in rats using a Sonos 4500 ultrasound system (Philips) with a 12 MHz linear array transducer.

Acipimox-enhanced FDG-PET was performed using a dedicated small animal PET system (MicroPET, Inveon, Siemens, Knoxville, TN, USA). LV end-diastolic volume (EDV), LV end-systolic volume (ESV) and LV ejection fraction (EF) were obtained from the set of contiguous ECG-triggered short-axis slices with the Quantitative Gated SPECT (QGS) software.

***In vivo* carotid mechanical properties**

We recorded simultaneously intra-arterial diameter and BP in isofluorane-anesthetized rats and mice using an ultrasonic echo-tracking device (NIUS-01, Asulab SA). The pressure measurement was made using a catheter (0.5 cm of polyethylene-10 fused to 3 cm of polyethylene-50) connected to a Statham pressure transducer (P23 Db) and a Gould pressure processor. The relation between the pressure and the lumen cross sectional area was fitted using an arc tangent function. Carotid cross sectional distensibility, a derivative of this function, was used to assess the global elastic behaviour of the artery. Circumferential wall stress (WS) and incremental elastic modulus (E_{inc}), which characterizes the intrinsic mechanical properties of the wall material, were calculated with the above-mentioned parameters and media cross sectional area (MCSA). To compare E_{inc}-WS curves, we calculated the mean WS (MWS) within the 350–2000 kPa range of E_{inc} for rats ($WS_{350-2000}$).

***Ex vivo* aorta mechanical properties**

Scanning acoustic microscopy (SAM) was conducted using a KSI 2000 microscope (PVA TePla Analytical Systems GmbH, Herborn, Germany) at 761 MHz on 5 µm thick cross-sections mounted on glass slides. The imaging was conducted using the newly developed multi-layer phase analysis (MLPA) method and the data was processed off-line to generate speed of sound maps for aorta sections from control and CT-1 animals (n=3 per group). Mean speed of sound values were determined with 1000 measurements per group. Furthermore, any differential contribution to stiffness within the aortic wall was investigated by determining the speed of sound for both the elastic lamellae and inter-lamellar regions (n=33 regions per group).

Aortic composition

Insoluble elastin, total collagen and cell protein contents were measured on descending thoracic aortae without homogenization, as described previously (Huang *et al.*, 1998). Briefly, aortic segments were opened longitudinally, the media separated from the adventitia and the medial length measured under a microscope. Media were then defatted, dried and their dry weight recorded. Medial cell proteins were extracted by 0.3% sodium dodecyl sulfate (SDS) and subsequently assayed and insoluble elastin was purified by the hot alkali method and quantified by weighing. Proteins in the NaOH extract were then hydrolysed, and total medial collagen was quantified by assaying hydroxyproline in the hydrolysate, using a colorimetric assay.

Histological evaluation

Histological determinations in cardiac, vascular and renal tissue were performed in 5 μm-thick sections. Sections were stained with haematoxylin for morphometry (cardiac and vascular), with Masson trichrome for cardiomyocyte dimensions (cardiac), with orcein for elastin content (vascular) and with Sirius red for collagen content (cardiac, vascular and renal). Media cross sectional area (MCSA) and glomeruli area were measured. For cell width and length, at least 30 cardiomyocytes per section were measured in triplicate. All measurements were performed blind in an automated image analysis system (Quancoul). Images were calibrated with known standards. Red-Sirius stained sections were analyzed under a microscope (40x), and all the fields covering the myocardial, vascular and the renal tissue section were digitized. Quantitative measurement of the area of perivascular fibrosis was calculated as the ratio of the area of fibrosis surrounding the vessel wall to the total vessel area. At least 10 arterial cross sections were examined per heart. The area of interstitial fibrosis or collagen deposition was identified after excluding the vessel area from the region of interest, as the ratio of interstitial fibrosis or collagen deposition to the total tissue area. For analyses of the glomerular and renal tubulointerstitial collagen volume fractions, 30 glomerular capsules and 30 fields without vessels or glomeruli were randomly selected from each kidney section, respectively. The glomerular and tubulointerstitial collagen volume fractions were then calculated as percentage of stained area within traced glomerular capsules and as percentage of total area within a field, respectively. All measurements were performed in an automated image analysis system (Quancoul) by two blinded observers. Images were calibrated with known standards.

Myocardial, vascular and renal sections (5 μm thick) were dewaxed and rehydrated, the slides were heated for 10 min in a solution containing 10 mM sodium citrate (pH 6.0) for CT-1, fibronectin, collagen type I, collagen type IV, β-catenin, E-cadherin and α-SMA immunodetection, incubated in 1% H_2O_2 for 10 min, and blocked with 5% normal goat serum in PBS for 1 h. Slides were incubated overnight with primary antibodies, washed three times, and then incubated for 30 min with the horseradish peroxidase-labeled polymer conjugated to secondary antibodies (Dako Cytomation, Carpentaria, CA). The signal was revealed by using diaminobenzidine chromagen substrate (Dako Cytomation), and the slides were counterstained with hematoxylin (Sigma-Aldrich).

Reverse transcription and real-time PCR

Total RNA extraction was performed using a nucleic acid purification lysis solution (Applied Biosystems) and the semiautomated ABI Prism 6100 Nucleic Acid PrepStation system (Applied Biosystems). Real-time PCR was performed with an ABI PRISM 7000 Sequence Detection System by using specific TaqMan MGB fluorescent probes (Applied BioSystems). Constitutive 18S ribosomal RNA was used as endogenous control.

Western Blot

Aliquots of 30 μg of proteins were size fractionated on polyacrylamide gels by electrophoresis. The following specific antibodies were used: CT-1 at 1:500 (Santa Cruz Biotechnology), Collagen type I at 1:1000 (Abcam), Collagen type III at 1:500 (Santa Cruz Biotechnology), Osteopontin at 1:500 (Abcam), Periostin at 1:500 (Abcam), TGF-β at 1:1500 (Cell Signaling), CTGF at 1:1000 (Santa Cruz Biotechnology), MMP-13 at 1:1000 (Millipore), MMP-3 at 1:500 (Millipore), Fibronectin at 1:500 (Millipore), elastin at 1:100 (Abcam), TIMP-1 at 1:500 (Santa Cruz Biotechnology), TIMP-3 at 1:500 (Santa Cruz Biotechnology), β-catenin at 1:1000 (Abcam), E-cadherin at 1:1000 (Abcam), α-SMA at 1:2000 (Sigma). Bound antibody was detected by peroxidase-conjugated secondary antibodies (Amersham Biosciences) and visualised using the ECL-Plus chemiluminescence detection system. After densitometric analyses, optical density values were expressed as arbitrary units (AU).

Zymography

Aliquots of 40μg of proteins were mixed with nonreducing sample buffer (Biorad) and fractionated by SDS-PAGE electrophoresis on a 10% gel containing 0.01% gelatine (Biorad).and fractionated by SDS-polyacrylamide gel electrophoresis on a 10% gel containing 0.1% gelatine (Bio-Rad) or casein (Bio-Rad). After electrophoresis, the gel was washed with renaturing buffer (2.5% Triton X-100) for 1 hour, before incubation for 24 hours at 37°C in a reaction buffer (50 mM Tris-HCl [pH 7.5], 5 mM $CaCl_2$, and 1% Triton X-100). The gel was then stained with Coomassie brilliant blue, and densitometric analyses were performed.

ELISA

Quantikine ELISA kits were used to measure albumin and creatinine (Abnova), NGAL (Interchim) and CT-1 (Cusabio) according to the manufacturer's protocols. All the samples were run in duplicate with the average of the 2 replicates reported.

Statistical Analysis

Results are presented as mean ± standard error of the mean and p values lower than 0.05 were considered significant. Comparisons between treatments or groups of animals were made by the unpaired Student's t test, the Mann Whitney U test or the repeated measures ANOVA, as appropriate.

SUPPLEMENTARY RESULTS

CT-1 receptors levels in CT-1-treated rats

Both gp130 and LIFR were spontaneously expressed in cardiac, vascular and renal tissues. Gp130 nor LIFR expressions were modified by CT-1 treatment at the mRNA or the protein levels in heart, aorta and kidney (Figure S1).

Renal fibrosis

To investigate the potential involvement of CT-1 in epithelial mesenchymal transition (EMT), expressions of both markers of myofibroblasts and epithelial cells were further analyzed. CT-1-infused rats presented an increase ($p<0.01$) of fibronectin and α-SMA content in kidney cortex as compared to vehicle (S4). Moreover, the expression of β-catenin and E-cadherin was lower ($p<0.01$) in the kidney of CT-1-infused rats as compared to controls (Figure S2). Taken together, these data indicate that the EMT phenotype was presented in kidneys from CT-1-treated rats and paralleled the fibrotic process as well as functional changes.

SUPPLEMENTARY TABLES

Table S1. Histological and molecular parameters of cardiac sections from CT-1-treated rats compared to control rats

Parameter	**Control**	**CT-1**
N	17	18
Cardiomyocyte length (µm)	84.3 ± 1.5	96 ± 2.5 *
Cardiomyocyte width (µm)	20.1 ± 0.3	19.3 ± 0.3
α-MHC (A.U.)	1.0 ± 0.15	2.1 ± 0.5 *
β-MHC (A.U.)	1.0 ± 0.12	2.0 ± 0.8 *
α-sarcomeric actin (A.U.)	1.0 ± 0.11	1.9 ± 0.7 *
MLC-1 (A.U.)	1.0 ± 0.18	1.7 ± 0.4 †
α-skeletal actin (A.U.)	1.0 ± 0.10	1.1 ± 0.1
MLC-2v (A.U.)	1.0 ± 0.11	0.8 ± 0.1

α-MHC, myosin heavy chain alpha; β-MHC, myosin heavy chain beta; MLC-1, myosin light chain-1, MLC-2v, myosin light chain-2v. * $p<0.01$ vs Control, †, $p<0.05$ vs Control

Table S2. Carotid artery and aortic parameters in CT-1-treated rats compared to control rats

Parameter	**Control**	**CT-1**
Carotid artery morphology		
N	10	9
MCSA ($\mu m^2\ 10^{-3}$)	101 ± 4	145 ± 6 *
Media thickness (µm)	41 ± 2	58 ± 3 *
Carotid diameter (mm)	1.20 ± 0.04	1.03 ± 0.03 *
Aortic composition		
N	10	10
Dry weight (mg/cm)	2.03 ± 0.15	2.39 ± 0.13 *
Cell proteins (% dry weight)	45 ± 5	58 ± 6 *
Cell proteins (mg/cm)	0.91 ± 0.1	1.33 ± 0.1 **
Elastin (% dry weight)	58 ± 4	59 ± 6
Elastin (mg/cm)	1.15 ± 0.06	1.39 ± 0.09
Collagen (% dry weight)	10 ± 0.6	13 ± 1 **
Collagen (mg/cm)	0.21 ± 0.01	0.31 ± 0.01 **
Aortic molecular parameters		
α1 integrin (A.U.)	1.0 ± 0.15	1.7 ± 0.5 †
α5 integrin (A.U.)	1.0 ± 0.13	1.9 ± 0.3 *
αv integrin (A.U.)	1.0 ± 0.15	1.8 ± 0.2 *
β1 integrin (A.U.)	1.0 ± 0.18	1.1 ± 0.2
β3 integrin (A.U.)	1.0 ± 0.20	1.7 ± 0.3 †
Vinculin (A.U.)	1.0 ± 0.13	2.2 ± 0.4 *
Talin (A.U.)	1.0 ± 0.12	1.8 ± 0.3 *
Fak-P/Fak (A.U.)	1.0 ± 0.14	1.6 ± 0.2 †

MCSA: media cross sectional area of the carotid artery; Fak: focal adhesion kinase. * $p<0.01$ vs Control, †, $p<0.05$ vs Control

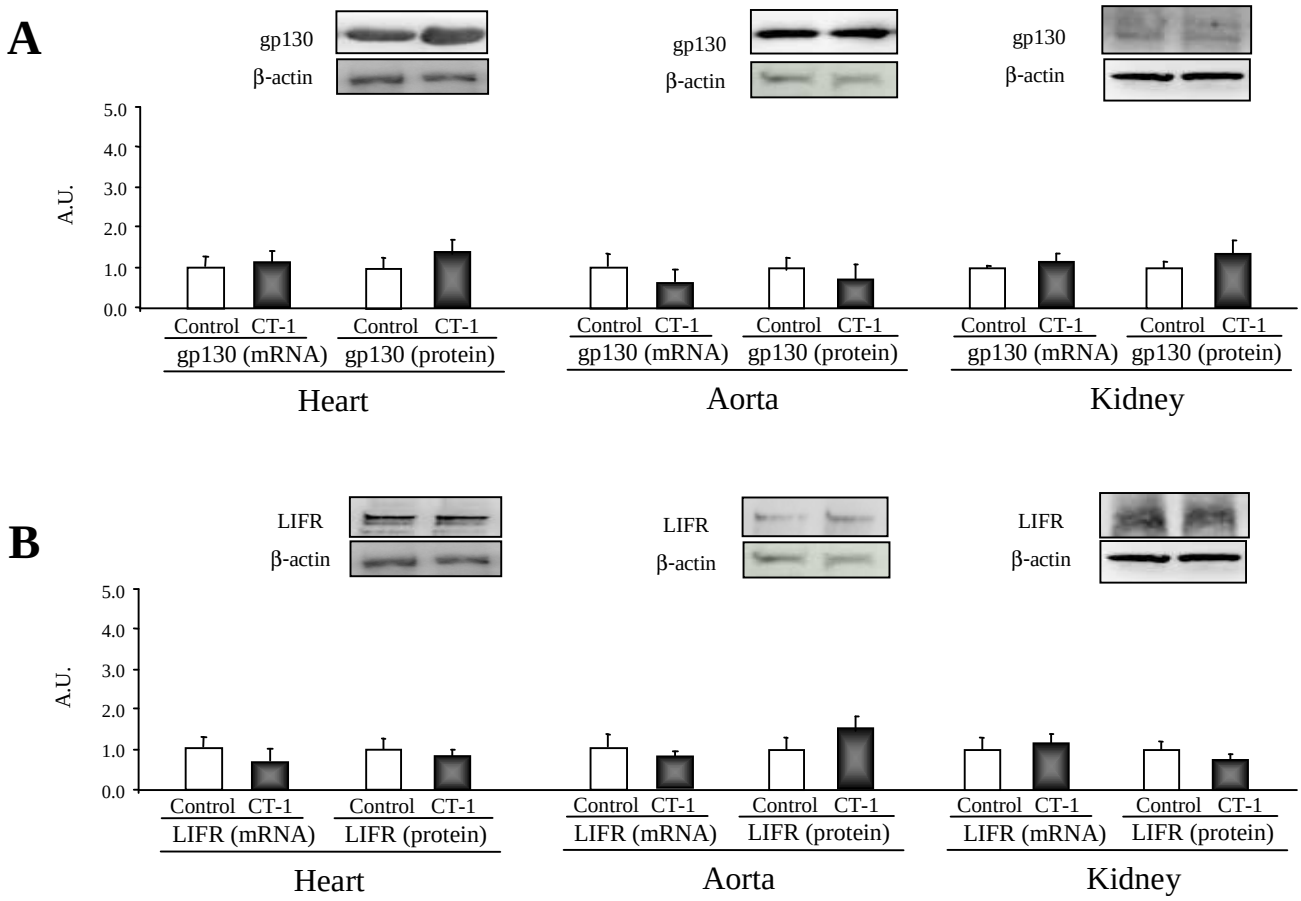

Figure S1. A, CT-1 treatment did not modify gp130 expression in heart, aorta and kidney. **B**, CT-1 treatment did not modify LIFR expression in heart, aorta and kidney. 18s gene expression or β-actin levels were used as loading controls in RT-PCR and Western blot respectively. Values are mean ± SEM.

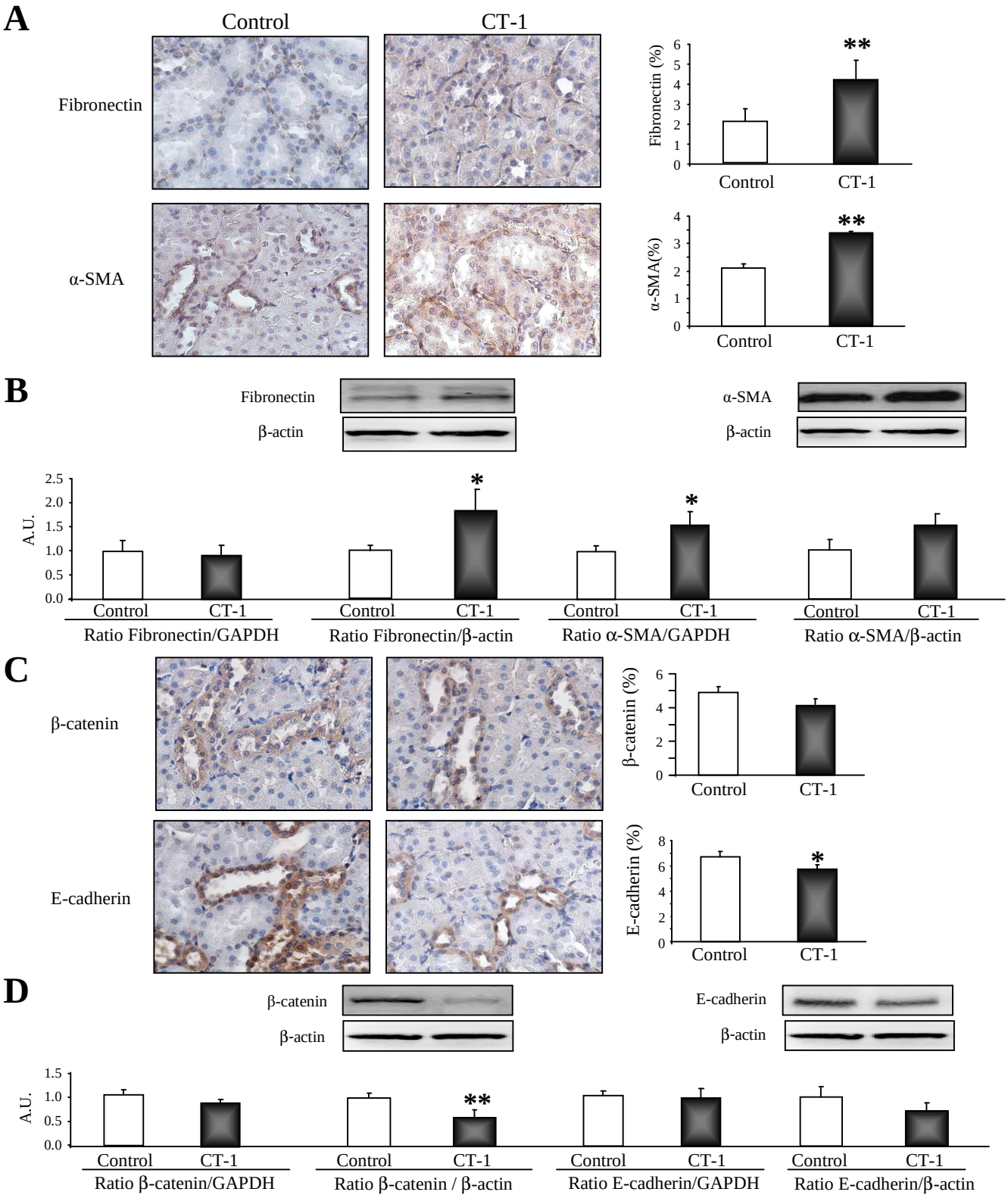

Figure S2. Epithelial-mesenchymal transition in control and CT-1-treated rats. A, Kidney from CT-1-treated rats presented increased fibronectin and α-SMA content by immunohistochemistry. **B**, CT-1-treated rats exhibited increased fibronectin protein expression, similar α-SMA protein expression, similar fibronectin mRNA expression and enhanced α-SMA mRNA expression as compared to controls. **C**, The kidney of CT-1-treated rats presented similar β-catenin content and a decrease of the E-cadherin content relative to controls. **D**, β-catenin and E-cadherin protein expressions were decreased as compared to controls, whereas mRNA expression was unchanged for the two genes. GAPDH expression or β-actin levels are used as loading controls in RT-PCR and Western blot respectively. Bars represent the mean ± SEM obtained from the two groups of animals (n=10 per group). *, $p<0.05$ vs Control; **, $p<0.01$ vs Control.